

Demonstration of an ultrahigh-sensitivity atom-interferometry absolute gravimeter

Zhong-Kun Hu,* Bu-Liang Sun, Xiao-Chun Duan, Min-Kang Zhou, Le-Le Chen, Su Zhan, Qiao-Zhen Zhang, and Jun Luo
*Ministry of Education Key Laboratory of Fundamental Physical Quantities Measurements, School of Physics,
 Huazhong University of Science and Technology, Wuhan 430074, People's Republic of China*
 (Received 28 April 2013; revised manuscript received 20 August 2013; published 8 October 2013)

We present an ultrahigh-sensitivity gravimeter based on an ^{87}Rb atom interferometer using stimulated Raman transitions. Compared with our previous work, a two-dimensional magneto-optical trap is added in the new gravimeter to increase the atom number and improve the detection signal-to-noise ratio, and a better optical phase-locked loop system is used to reduce the phase noise of Raman beams. Benefiting from these efforts and the excellent performance of the active vibration isolator, a short-term sensitivity of about $4.2 \mu\text{Gal}/\sqrt{\text{Hz}}$ ($1 \mu\text{Gal} = 1 \times 10^{-8} \text{ m/s}^2$) is reached, which improves the sensitivity by a factor of 2 compared with the former best reported value. By a modulation experiment, we further indicate that the residual vibration noise contribution is about $1.2 \mu\text{Gal}/\sqrt{\text{Hz}}$, which implies a possible improvement over the present absolute gravity measurement level by about one order of magnitude. Moreover, we demonstrate a calibration experiment to directly evaluate the sub- μGal resolution of our gravimeter.

DOI: [10.1103/PhysRevA.88.043610](https://doi.org/10.1103/PhysRevA.88.043610)

PACS number(s): 37.25.+k, 03.75.Dg, 04.80.Cc

I. INTRODUCTION

In the last two decades, atom interferometry techniques have been rapidly developed and widely used, of which performances compete with other state of the art techniques [1–3]. This technology has been widely used to measure the local gravity [4–8], gravity gradient [9,10], rotation [11,12], fine-structure constant [13], magnetic-field gradient [14,15], and Newtonian gravitational constant [16,17] and to test fundamental laws of physics [18–22].

Among these, gravimeters are of great interest for a wide range of essential applications, from geophysics to fundamental physics to metrology. Steve Chu's group has achieved a sensitivity of $8 \mu\text{Gal}/\sqrt{\text{Hz}}$ [20], which exceeds that of the classic corner cube gravimeter [23,24] and has ever since been the best reported value in the literature. Both for scientific research and practical applications, it is a pressing need to improve the sensitivity of gravimeters. Recently, progress in increased momentum transfer [25–31] or pulse separation time [32] has been reported to enhance the measurement signal. However, in high-precision absolute gravity measurement, the vibration noise is still an obstacle and its influence cannot be alleviated by simply increasing the signal.

In order to precisely measure the absolute gravity acceleration, cold atom gravimeters using a typical $\pi/2\text{-}\pi\text{-}\pi/2$ pulse Raman sequence have been built in our cave laboratory since 2006 [33]. Compared with the works mentioned above, our goal is to reach a sensitivity of a few $\mu\text{Gal}/\sqrt{\text{Hz}}$ by suppressing the main noises in the experiment. This highly sensitive gravimeter can be used for precision gravitational experiments, such as determining the Newtonian gravitational constant G and testing equivalence principle. In our previous work [8], an active vibration isolator with a natural resonance frequency of about 0.016 Hz was demonstrated and the residual vibration noise contribution was estimated to be about $1 \mu\text{Gal}/\sqrt{\text{Hz}}$. However, we achieved only a sensitivity of about $55 \mu\text{Gal}/\sqrt{\text{Hz}}$, which is much higher than the residual

vibration noise contribution due to other noises, such as detection noise and Raman phase noise.

In this work, by employing a two-dimensional magneto-optical trap (2D-MOT), a low-noise optical phase-locked loop (OPLL), and an adjustable active feedback vibration isolator to further suppress measurement noise, we achieve a sensitivity of $4.2 \mu\text{Gal}/\sqrt{\text{Hz}}$ for absolute gravity measurement, which to our knowledge is the best reported value. The corresponding resolution with a 100-s integration time is better than $0.5 \mu\text{Gal}$, which is directly approved by a calibration experiment using attracting masses to produce an additional gravitational acceleration. Moreover, a modulation experiment is implemented to further indicate that the residual vibration noise contribution is about $1.2 \mu\text{Gal}/\sqrt{\text{Hz}}$.

II. EXPERIMENTAL SETUP

The principle of an atom gravimeter based on two-photon stimulated Raman transitions has been described in detail in Ref. [13]. It utilizes a $\pi/2\text{-}\pi\text{-}\pi/2$ Raman-pulse sequence to coherently split, reflect, and finally combine the atomic wave packet. After that sequence, the mean transition probability P of the atoms is determined by the interferometer's phase shift $\Delta\Phi$ as $P = (1 + C \cos \Delta\Phi)/2$, where C is the visibility of the interferometry fringe. Without considering the effect of the gravity gradient, the phase shift $\Delta\Phi$ can be expressed as

$$\Delta\Phi = (\vec{k}_{\text{eff}} \cdot \vec{g} - \alpha)T^2, \quad (1)$$

where g is the local gravitational acceleration due to the Earth, T is the separation time between two pulses, $\vec{k}_{\text{eff}} = \vec{k}_1 - \vec{k}_2$ is the effective wave vector, and α is the chirp rate of the Raman beams. The chirp rate is adjusted to compensate the Doppler shift induced by the free falling atoms. We can scan the α in a constant step to get the interferometry fringe, by the sine fitting of which the value of g can be obtained. In the measuring process, phase noise of the Raman beams, vibration noise, and detection noise will cause fluctuations of the transition probability, which will show up as the fluctuations of the measured

*zkhu@mail.hust.edu.cn

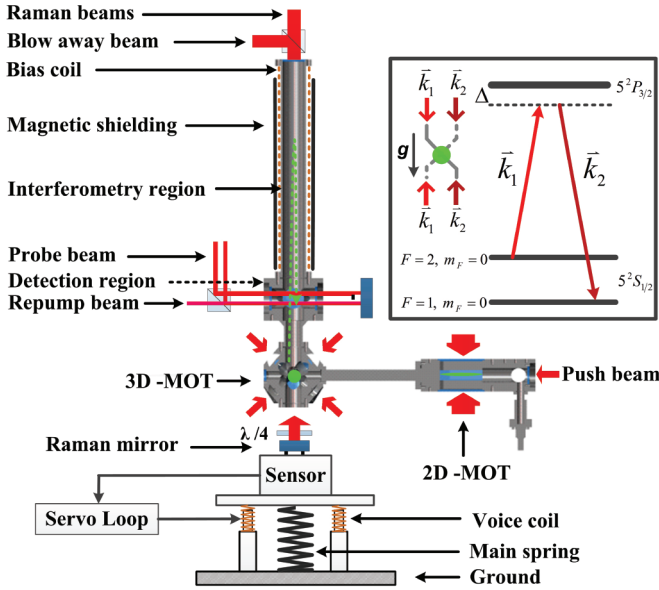


FIG. 1. (Color online) Schematic experimental setup of our atom gravimeter. The Λ -type structure of stimulated Raman transition and the propagation of the Raman beams are shown in the inset.

gravitational acceleration. It is very important to suppress these main noises in high-precision gravity measurement.

A. Apparatus

The experimental setup is schematically shown in Fig. 1, which is similar to that of our previous system [8] except for several changes to improve the performance. First, the vacuum chamber is made of titanium instead of aluminum to reduce the effect of eddy current. Second, the distance between the interference tube and three-dimensional magneto-optical trap (3D-MOT) is reduced, so that a pulse separation time of 300 ms is available rather than the previous time of 200 ms for similar fountain heights. Third, in the atom trap stage, a 2D-MOT with a push beam is used to increase the loading rate of the 3D-MOT while keeping its high vacuum. The 3D-MOT with a 1-1-1 configuration is located 27 cm horizontally downstream from the 2D-MOT and linked with a differential pump. When the system is working, the vacuum pressure in the 2D-MOT and the 3D-MOT chamber is about 10^{-8} and 10^{-10} Torr, respectively. The cold atom loading rate in 3D-MOT can reach up to about 1×10^{10} atoms/s, which is about one order of magnitude higher compared with our previous result. In our current experiment, about 3×10^9 atoms are trapped within 200 ms. The trapped atoms are then launched with an initial velocity of about 3.83 m/s, corresponding to a flight apex of about 0.75 m relative to the MOT center. After the atoms entered the interferometry region, a Raman π pulse with a duration of $12 \mu\text{s}$ is switched on to select atoms in the magnetic-insensitive sublevel and in a narrow region of vertical velocity distribution. With this process, about 5×10^7 atoms with a vertical temperature of about 300 nK are prepared in the $F = 1, m_F = 0$ state. Afterward, the interferometer is realized with a $\pi/2$ - π - $\pi/2$ Raman pulse sequence, which is separated by a free evolution time of T . Finally, we get the transition probability through a fluorescence measurement

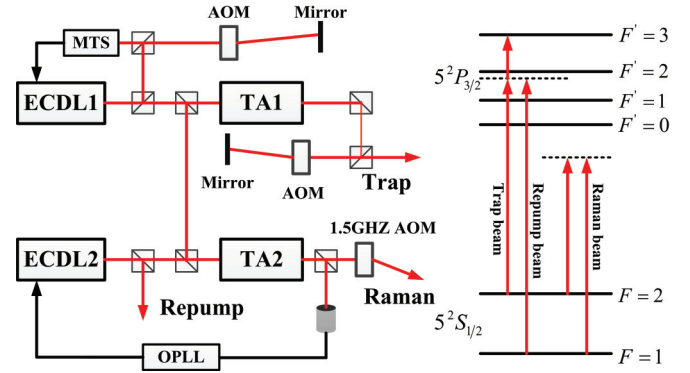


FIG. 2. (Color online) Optical setup in our experiment. The detection and blow away beams are also produced by TA1 and not shown here. ECDL, extended cavity diode laser; TA, tapered amplifier; AOM, acoustic-optic modulators; MTS, modulation-transfer stabilized; OPLL, optical phase-locked loop.

of the population of atoms in $F = 2$ and 1 states by the normalized detection method. The whole time used for a single measurement is 1 s.

B. Optical setup

The laser including cooling and Raman beams used in our experiment are produced by a robust laser system, which contains two extended cavity diode lasers (ECDLs: Toptica DL pro) and two tapered amplifiers (TAs: Toptica BoosTA), as shown in Fig. 2. The ECDL1 is locked on the transition of $5S_{1/2}, F = 2 \rightarrow 5P_{3/2}, F' = 3$ by the modulation-transfer stabilized (MTS) method after a frequency shift of 270 MHz by acoustic optical modulators (AOMs: AA MT.110). Then it is amplified to 1 W and shifted about 250 MHz to produce the cooling beams for 2D-MOT and 3D-MOT. The ECDL2 is split into two paths, one of which is used as repumping beams in the loading and detection process, and the other is combined with a part of light from ECDL1. The combined beam is amplified to 800 mW and shifted by 1.5 GHz with an AOM (Brimrose GPF-1500-200-.780) to produce the Raman beams. The ECDL2 is phase locked to ECDL1 by a home-made optical phase-locked loop (OPLL) with a frequency offset of 6.834 GHz. By feeding the error signal back to the ECDL2 via three feedback paths (one path for PZT, two paths for current), the corresponding bandwidth of OPLL is about 2 MHz, and the phase noise of the laser beat note in the region of 200 Hz to 200 kHz is less than -100 dBc/Hz measured by a phase noise analyzer (Agilent E5505A), which is shown in Fig. 3. The phase noise of low frequency (less than 100 Hz) is dominant limited by the 6.834-GHz reference. The Raman beams are overlapped and are coupled into one single fiber before entering the vacuum chamber, which can reduce the noise accrued in the transferring path.

A retroreflector, denoted as the Raman mirror in Fig. 1, is placed under the MOT chamber, which is necessary to realize the counterpropagating configuration by retroreflecting the Raman beams, and there are two pairs of counterpropagating Raman beams in the vertical direction. However, due to the Doppler shift produced by the free falling atom, only one pair

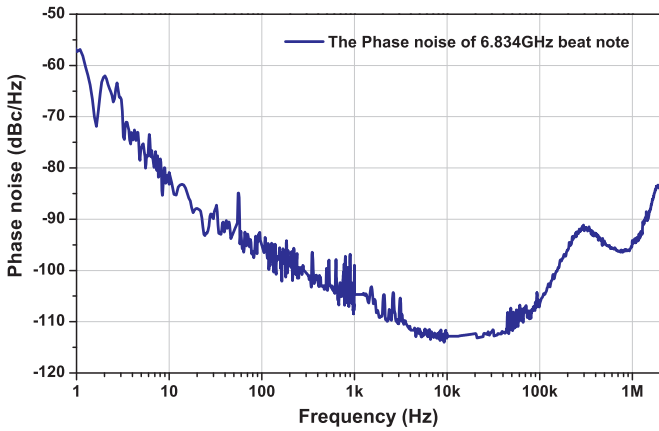


FIG. 3. (Color online) Single sideband phase noise of 6.834 GHz beat note signal.

of Raman beams can satisfy the resonant condition by scanning the Raman laser frequency of about 25.14 MHz/s.

III. EXPERIMENT

A. Gravity measurement

In our experiment, the interferometry fringe is obtained by slightly changing α with a constant step. Figure 4 shows a typical fringe for a pulse separation time of 300 ms, which contains 40 shots in 40 s. The least-squares sine fitting of the fringe gives an uncertainty of about 11 mrad, which corresponds to a resolution of about $0.8 \mu\text{Gal}$ in 40 s. By modulating the central fringe with a phase shift of $\pm\pi/2$, we can get an error signal, which is then used to lock the chirp rate of the Raman beam to the fringe center with a digital servo loop [34]. This can be used to give a high-rate gravity measurement of a 2-s interval with a sensitivity better than the method of fringe fitting.

In order to evaluate the long-term stability of our gravimeter, a continuous g measurement is carried out for 40 h, as shown in Fig. 5(a). Each point represents two shots in every 2 s. The experimental data are consistent with the theoretical model of the Earth's tide. The residual acceleration by subtracting the theory model from the experimental data is

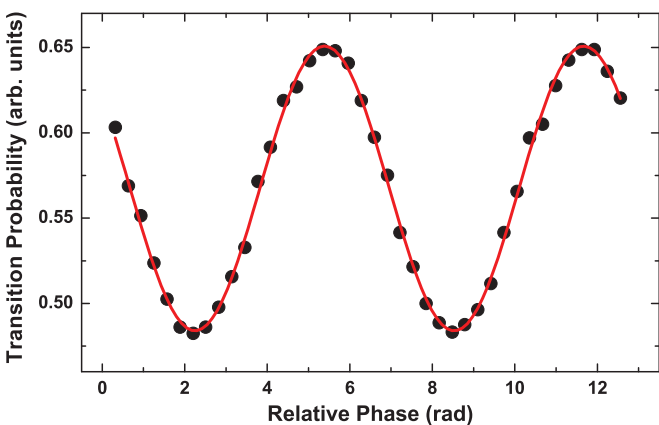


FIG. 4. (Color online) Typical interferometry fringe for a pulse separation of 300 ms, where the fringe shows 40 shots for 40 s.

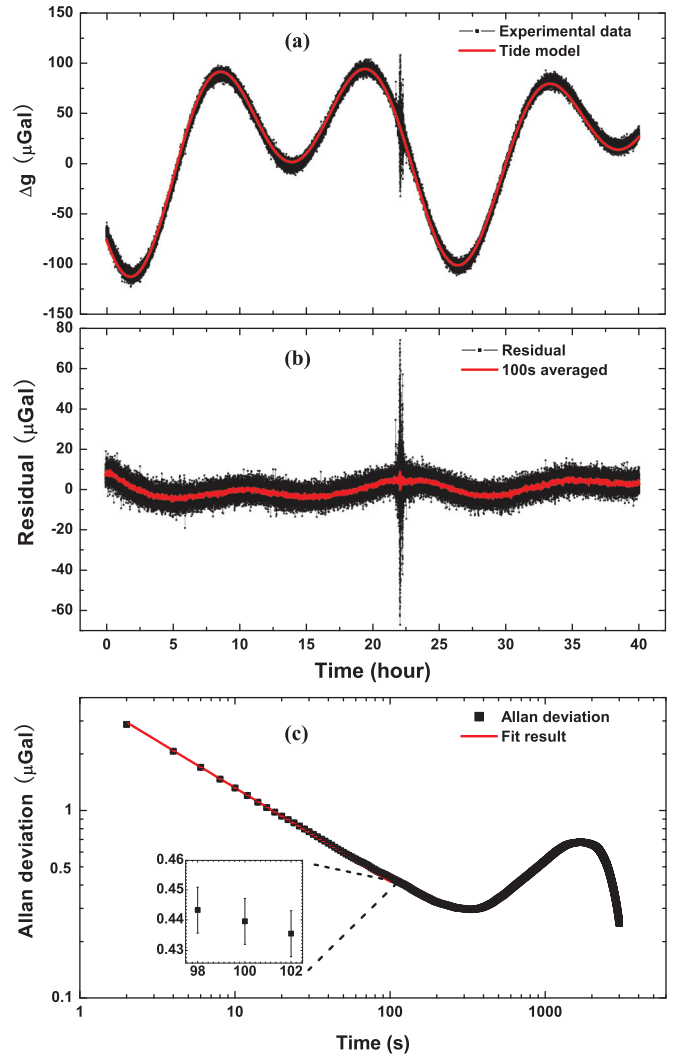


FIG. 5. (Color online) (a) Continuous gravity measurement of 40 h operated by our gravimeter between 14 and 16 April 2013. Each data point represents two shots in 2 s. The red line is the theory model of the Earth's tide. (b) The residual acceleration by subtracting the theory model from the experimental data. (c) Allan deviation of the g measurement calculated from the residual acceleration. The red solid line corresponds to a short-term sensitivity of $4.2 \mu\text{Gal}/\sqrt{\text{Hz}}$.

shown in Fig. 5(b). Seismic waves produced by the earthquake of magnitude 6.6 that occurred in Papua New Guinea on 14 April 2013 are clearly shown in our measurement. The Allan deviation of the gravity measurements is calculated from the residual acceleration, which is shown in Fig. 5(c). The short-term sensitivity up to 100 s given by the Allan deviation is $4.2 \mu\text{Gal}/\sqrt{\text{Hz}}$, as shown in the figure by the red solid line. After an integration time of 100 s, the resolution is better than $0.5 \mu\text{Gal}$, as shown in the inset of Fig. 5(c). We have observed a fluctuation of the room temperature in our experiments, which may account for the bump in the Allan deviation at about 2000 s as shown in Fig. 5(c).

B. Resolution calibration

Due to the imperfection of the present theoretical tide model at our laboratory site, it is insufficient to evaluate the short-term

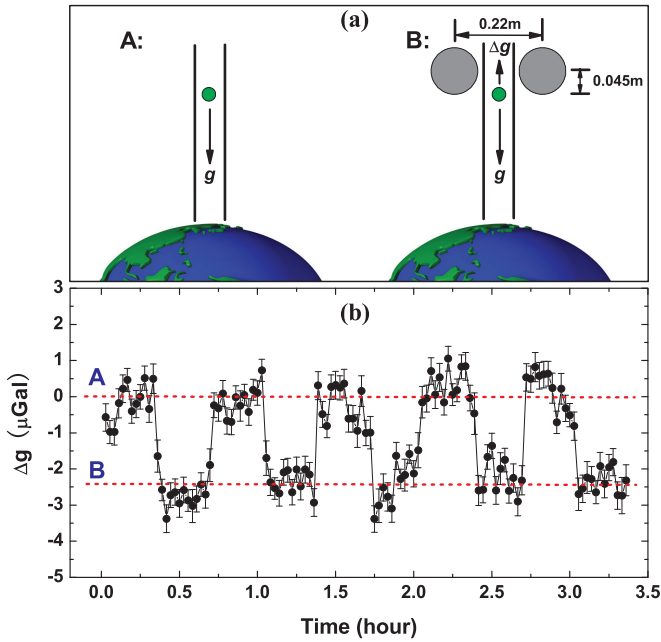


FIG. 6. (Color online) (a) The sketch map of the gravity calibration experiment. (b) The result of the gravity calibration experiment by moving the attracting mass on and off the position. Each point is a statistical average of 50 measurements with a time of 100 s. A and B in both figures represent the cases of the attracting masses off and on the position, respectively.

sensitivity by comparing the measurement result with the theoretical tide model when the precision of gravimeters gets higher and higher. Based on the idea of measuring G , we utilize well-machined test masses to produce desired additional gravitational acceleration to help evaluate the resolution of our gravimeter. As shown in Fig. 6(a), two stainless steel SS316 spheres with an individual mass of 8.55 kg are placed around the interferometry region symmetrically and with a vertical distance of 0.045 m above the apex of the atom parabola. The spheres are from the same batch of test masses that was used for measuring G in our cave laboratory [35] and will produce a theoretical gravitational acceleration shift with an effective mean value of $(2.26 \pm 0.07) \mu\text{Gal}$ here. By moving the spheres on and off the position with a period of about 40 min, the corresponding acceleration changes can be obtained from the continued gravity acceleration measurement.

Figure 6(b) shows the result of the calibration experiment by subtracting the tide effect. Each point is a statistical average of 50 measurements with a time of 100s, the standard deviation of each point is less than $0.5 \mu\text{Gal}$, which is consistent with the Allan deviation result. The experiment result gives a shift of $(2.49 \pm 0.26) \mu\text{Gal}$ and agrees with the theoretical calculation. This experiment directly demonstrated that the resolution of our atom gravimeter is better than $0.5 \mu\text{Gal}$ in 100-s integration time.

C. Vibration noise modulation

In a high-sensitivity absolute gravimeter, the vertical vibration is usually a dominant noise source as a result of the equivalence principle. Suppressing the residual vibration

noise of the Raman mirror is a key issue to achieve such high resolution in our gravimeter. The active vibration isolator used here is similar to our previous one demonstrated in Ref. [8]. It utilizes a seismometer to sense the vibration on a passive isolator, of which the output is used as an error signal for feedback to voice-coil type actuators to further reduce the residual vibration noise of the platform. For this active vibration isolation system, the vibration noise in the frequency region higher than 10 Hz gets worse with high feedback gain. We find an optimized relative feedback gain of about 3 for the active isolator in our gravimeter. Thus it is capable of changing the level of the residual vibration noise by setting the relative feedback gain between 0 and 3, which is adopted to verify the influence of vibration in our gravimeter. The corresponding typical vertical vibration noises with different relative feedback gains are measured and are shown in Fig. 7(a). It shows that the vibration noise can be suppressed by about 10 dB in the frequency region higher than 2 Hz with only a passive isolator, while at its natural resonance frequency of about 0.8 Hz the vibration noise is increased. The vibration noise in the frequency region of about 0.1 to 10 Hz

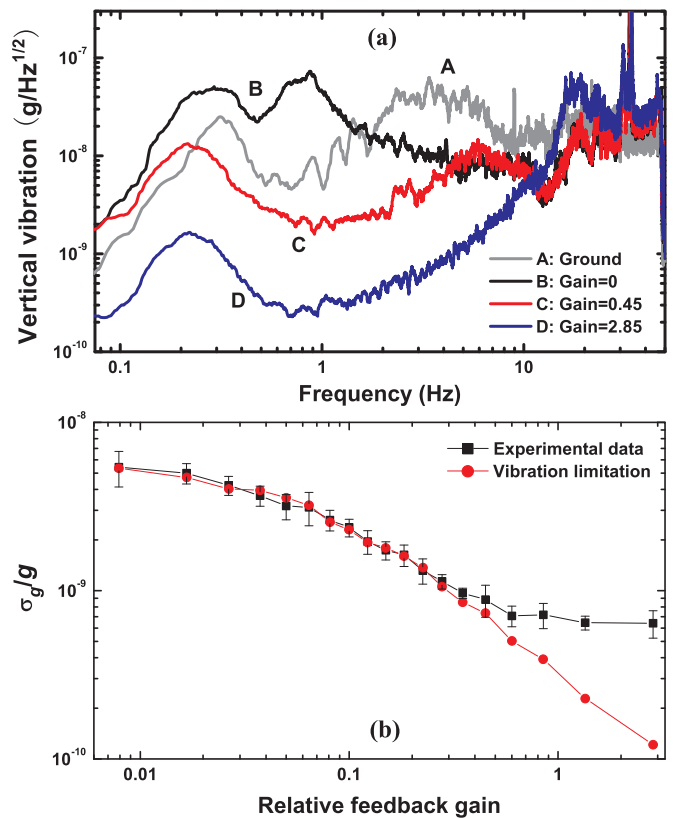


FIG. 7. (Color online) (a) Vertical vibration noise of different relative feedback gains measured by the seismometer (Guralp CMG-3ESP). The black line is the ground vibration noise in our cave laboratory. A total of 19 experiments with different vibration levels are carried out, and only three of them are shown here. (b) The resolution of the g measurement (the square points with error bar) with different noise levels of the active vibration isolator, which agrees well with the theory calculation of vibrational noise limitation (the red circle points). Each point in (b) is the deviation with an integration time of 100 s.

can be suppressed by about 20 dB with a relative feedback gain of 2.85.

With these vibration noise data, we can calculate theoretically the limitation due to different vibration noise levels by the equation [6]

$$\sigma_g^2(\tau) = \frac{4}{T^4} \int_0^\infty \frac{\sin^4(\pi f \tau)}{\sin^2(\pi f T_{\text{rep}})} |G(f)|^2 \frac{S_a(f)}{(2\pi f)^2} df, \quad (2)$$

where τ is the integration time, T_{rep} is the time for one shot, $S_a(f)$ is the power spectral density of the vibration noise, and $G(f)$ is the Fourier transformation of the sensitive function. The gravity measurements with an integration time of 100 s under different vibration conditions are measured and compared with these theoretical calculations of vibration contribution, which are shown in Fig. 7(b). We find that the experimental data agree with the theoretical calculation very well when the residual vibration noise dominates. This indicates that the resolution of our gravimeter is no longer limited by the vibration noise at the level of about 0.5 μGal in our current experiment, and the resolution limit due to residual vibration noise will be at a level of 0.1 μGal with an integration time of 100 s.

IV. DISCUSSION AND CONCLUSION

Besides the vertical vibration noise, other noise sources, such as phase noise of the Raman beams and detection noise, also contribute noise to our gravity measurements. For the Raman beams' phase noise in our gravimeter, the corresponding noise contribution is about 0.8 $\mu\text{Gal}/\sqrt{\text{Hz}}$. To evaluate the contribution of the detection noise, we measure the fluctuation of transition probability versus different atom numbers by changing the loading time. In our current experiment, the loading time is set at 200 ms, and the corresponding standard deviation of transition probability σ_P is about 0.0035. This gives a limitation of the resolution as $\sigma_g = 2\sigma_P/Ck_{\text{eff}}T^2$ per

shot, which is about 3.3 $\mu\text{Gal}/\sqrt{\text{Hz}}$, while considering a fringe visibility of about 15% and a pulse separation time of 300 ms. This is mainly induced by the frequency and intensity noise of the probe beam. Further work including robust frequency stabilization and active feedback stabilization of the intensity will be implemented in our future experiment.

In conclusion, a sensitivity of 4.2 $\mu\text{Gal}/\sqrt{\text{Hz}}$ on our atom gravimeter is thus achieved by the increase of the cold atom number and the employment of a lower noise Raman beam together with an active vibration isolator to suppress the seismic noise. With an integration time of 100 s, the resolution is better than 0.5 μGal , which is directly proven by the gravitational calibration experiment using two attracting masses. The vibration modulation experiment further indicates that the vibration noise contribution in our gravimeter can be decreased to a level of about 1.2 $\mu\text{Gal}/\sqrt{\text{Hz}}$, which gives a potential resolution that advances the present absolute gravity measurements by about one order of magnitude. All of these works provide the basic groundwork for absolute measurement with a level of 0.1 μGal at a short time of 100 s. Such a high-precision absolute gravimeter could be used to calibrate a relative gravimeter at a level of 0.1 μGal and be applied to high-precision fundamental physical experiments, which can effectively avoid the influence of long time environmental fluctuation noises.

ACKNOWLEDGMENTS

We thank Zehuang Lu, Jie Zhang, Zebing Zhou, and Chenggang Shao for enlightening discussions and technical support in this experiment. We also owe thanks to Shanqing Yang and Chao Xue for their help with the gravity calibration experiment. This work is supported by the National Natural Science Foundation of China (Grants No. 41127002, No. 11205046, and No. 11204094) and the National Basic Research Program of China (Grant No. 2010CB832806).

-
- [1] F. Riehle, T. Kisters, A. Witte, J. Helmcke, and C. J. Bordé, *Phys. Rev. Lett.* **67**, 177 (1991).
 - [2] M. Kasevich and S. Chu, *Phys. Rev. Lett.* **67**, 181 (1991).
 - [3] C. J. Bordé, *Metrologia* **39**, 435 (2002).
 - [4] A. Peters, K. Y. Chung, and S. Chu, *Nature (London)* **400**, 849 (1999).
 - [5] A. Peters, K. Y. Chung, and S. Chu, *Metrologia* **38**, 25 (2001).
 - [6] J. Le Gouët, T. E. Mehlstäubler, J. Kim, S. Merlet, A. Clairon, A. Landragin, and F. Pereira Dos Santos, *Appl. Phys. B* **92**, 133 (2008).
 - [7] M. Schmidt, A. Senger, M. Hauth, C. Freier, V. Schkolnik, and A. Peters, *Gyroscopy and Navigation* **2**, 170 (2011).
 - [8] M. K. Zhou, Z. K. Hu, X. C. Duan, B. L. Sun, L. L. Chen, Q. Z. Zhang, and J. Luo, *Phys. Rev. A* **86**, 043630 (2012).
 - [9] M. J. Snadden, J. M. McGuirk, P. Bouyer, K. G. Haritos, and M. A. Kasevich, *Phys. Rev. Lett.* **81**, 971 (1998).
 - [10] J. M. McGuirk, G. T. Foster, J. B. Fixler, M. J. Snadden, and M. A. Kasevich, *Phys. Rev. A* **65**, 033608 (2002).
 - [11] T. L. Gustavson, A. Landragin, and M. A. Kasevich, *Class. Quantum Grav.* **17**, 2385 (2000).
 - [12] D. S. Durfee, Y. K. Shaham, and M. A. Kasevich, *Phys. Rev. Lett.* **97**, 240801 (2006).
 - [13] D. S. Weiss, B. C. Young, and S. Chu, *Appl. Phys. B* **59**, 217 (1994).
 - [14] M. K. Zhou, Z. K. Hu, X. C. Duan, B. L. Sun, J. B. Zhao, and J. Luo, *Phys. Rev. A* **82**, 061602 (2010).
 - [15] Z. K. Hu, X. C. Duan, M. K. Zhou, B. L. Sun, J. B. Zhao, M. M. Huang, and J. Luo, *Phys. Rev. A* **84**, 013620 (2011).
 - [16] J. B. Fixler, G. T. Foster, J. M. McGuirk, and M. A. Kasevich, *Science* **315**, 74 (2007).
 - [17] F. Sorrentino, Y. H. Lien, G. Rosi, G. M. Tino, L. Cacciapuoti, and M. Prevedelli, *New J. Phys.* **12**, 095009 (2010).
 - [18] S. Fray, C. A. Diez, T. W. Hänsch, and M. Weitz, *Phys. Rev. Lett.* **93**, 240404 (2004).
 - [19] G. Tino and F. Vetrano, *Class. Quantum Grav.* **24**, 2167 (2007).
 - [20] H. Müller, S. W. Chiow, S. Herrmann, S. Chu, and K. Y. Chung, *Phys. Rev. Lett.* **100**, 031101 (2008).

- [21] P. W. Graham, J. M. Hogan, M. A. Kasevich, and S. Rajendran, *Phys. Rev. Lett.* **110**, 171102 (2013).
- [22] S. Y. Lan, P. C. Kuan, B. Estey, D. English, J. M. Brown, M. A. Hohensee, and H. Müller, *Science* **339**, 554 (2013).
- [23] T. Niebauer, G. Sasagawa, J. Faller, R. Hilt, and F. Klopping, *Metrologia* **32**, 159 (1995).
- [24] J. Faller, *Metrologia* **39**, 425 (2002).
- [25] J. M. McGuirk, M. J. Snadden, and M. A. Kasevich, *Phys. Rev. Lett.* **85**, 4498 (2000).
- [26] S.-W. Chiow, T. Kovachy, H.-C. Chien, and M. A. Kasevich, *Phys. Rev. Lett.* **107**, 130403 (2011).
- [27] E. M. Rasel, M. K. Oberthaler, H. Batelaan, J. Schmiedmayer, and A. Zeilinger, *Phys. Rev. Lett.* **75**, 2633 (1995).
- [28] P. Cladé, S. Guellati-Khélifa, F. Nez, and F. Biraben, *Phys. Rev. Lett.* **102**, 240402 (2009).
- [29] H. Müller, S. W. Chiow, S. Herrmann, and S. Chu, *Phys. Rev. Lett.* **102**, 240403 (2009).
- [30] T. Lévèque, A. Gauguet, F. Michaud, F. Pereira, Dos Santos, and A. Landragin, *Phys. Rev. Lett.* **103**, 080405 (2009).
- [31] N. Malossi, Q. Bodart, S. Merlet, T. Lévè que, A. Landragin, and F. Pereira Dos Santos, *Phys. Rev. A* **81**, 013617 (2010).
- [32] S. M. Dickerson, J. M. Hogan, A. Sugarbaker, D. M. S. Johnson, and M. A. Kasevich, *Phys. Rev. Lett.* **111**, 083001 (2013).
- [33] M. K. Zhou, Z. K. Hu, X. C. Duan, B. L. Sun, J. B. Zhao, and J. Luo, *Front. Phys. China* **4**, 170 (2009).
- [34] P. Cheinet, F. Pereira, Dos Santos, T. Petelski, J. Le. Gouët, J. Kim, K. T. Therkildsen, A. Clairon, and A. Landragin, *Appl. Phys. B* **84**, 643 (2006).
- [35] J. Luo, Q. Liu, L. C. Tu, C. G. Shao, L. X. Liu, S. Q. Yang, Q. Li, and Y. T. Zhang, *Phys. Rev. Lett.* **102**, 240801 (2009).